Proceedings of HP1, IAHS-IAPSO-IASPEI Assembly, Gothenburg, Sweden, July 2013 (IAHS Publ. 358, 2013).

Monitoring flood propagation in the Niger River Inner Delta in Mali: prospects with the low resolution NOAA/AVHRR data

ADAMA MARIKO[1], GIL MAHE[2] & DIDIER ORANGE[3]

1 Ecole Nationale d'Ingénieurs Abderhamane Baba Touré (ENI-ABT), BP 242, Bamako, Mali
adama.mariko@ird.fr

2 IRD, Université Mohamed V Agdal, BP 8967, 10 000 Rabat Agdal, Morocco

3 IRD, LBI, Univ. Paris VI, Box 120, 4 place Jussieu, 75 252 Paris cedex 10, France

Abstract The low resolution NOAA/AVHRR$_{14}$ data is used to characterize the space–time propagation of the flood and of the vegetation cover in the Inner Delta of the Niger River in Mali. We propose a method to identify the inundation front on satellite images, and to discriminate pixels of open water, flooded vegetation, vegetation on dry soil and bare soil. From the analysis of four images, taken at different dates well representing the whole cycle of water regime (from the filling to the emptying of the flood plain), we identify the four significant vegetative stages during the annual cycle: bare soil, vegetation on dry soil, flooded vegetation, open water. A selection of indexes sensitive to water surfaces and vegetation cover are presented. Then we propose an analysis of spectral signatures with a visual examination of coloured compositions to finally locate these four classes of pixels during the annual evolution of the flood.

Key words flood monitoring; open water; flooded vegetation; AVHRR; River Niger; Inner Delta; Mali

INTRODUCTION

Flooding of the Niger River's Inner Delta (NRID) depends on the annual rainfall in the Upper Niger Basin (UNB) (Conway & Mahe, 2009; Mahe *et al.*, 2009). It plays a main role in the natural resources productivity, i.e. fisheries, pastures and cultivations (Poncet & Orange, 1999), so the water management in this area is a high priority (Ogilvie *et al.*, 2010; Mulligan *et al.*, 2011). However, the forecast of the flood in the Delta is necessary to carry out chart sets for the natural resources management. Remote sensing data are very useful in that case.

The 10-days synthesis of the NOAA/AVHRR images acquired by the Agrhymet Centre in Niamey (Niger) is used to identify the space–time propagation of the flood in the NRID, through the monitoring of four main items: open water, floating vegetation, vegetation on dry soil and bare soil. These land surfaces present rather different behaviours in the solar and thermal spectral fields. The open water or water mixed with vegetation, contrary to the other items, is characterized by weak numerical accounts in thermal spectral field. The vegetation has a more reflective capacity in the infrared than in the visible wave lengths, and is distinguished from the bare soils which present a reverse effect in the same spectral fields. In this study, we propose to carry out a discrimination of these four items, corresponding to the four main land cover types in the NRID, by the spectral behaviour analysis of each one.

We build the indexes from the decomposition of the spectral signatures of various observed items, which allows their identification on the colour composite images (Jackson, 1983; Townshend & Justice, 1986; Justice & Hiernaux, 1986). For example, the NDVI index (Normalised Difference Vegetation Index, Jackson, 1983) allows the identification of vegetation on colour composite images. The knowledge of spectral behaviours in the arid land has been improved by Smith *et al*. (1990), etc. while the known indexes are used to highlight the presence of simple items like water, vegetation and bare soil, the use of this index still remains very limited for the identification of complex items like the flooded vegetation, which occupies >70% of our study area.

After a comparative study of the existing indexes, new indexes are developed to ensure better mapping and the space–time monitoring of the flood in the NRID.

THE NIGER RIVER INNER DELTA

Located in the Sahelian semi-arid climatic zone, NRID is a vast flooded area of about 40 000 km^2 stretched over more than 350 km (Fig. 1). It is composed of a very dense network of

interconnected channels and small rivers supplied by the Niger River (NR) and its tributary the Bani River (BR) (Lienou *et al.*, 2010), which joins it at Mopti. Annual rainfall varies from 600 mm in the south to 300 mm in the north (Mahe *et al.*, 2011). The UNB extends over 249 000 km^2 in Guinea, northern Ivory Coast and the south of Mali.

The flood occurs each year between July and December and depends on the hydrological regimes of the NR and BR, which both contribute to >90% of the water input in the Delta, local rainfall on the Delta accounting for only a minor fraction (Mahe *et al.*, 2009). Flood propagation time is very variable. It depends on the absolute water level: it is longer the more the maximum level is high (Olivry, 1995). Between the minimum and maximum levels, the propagation time can vary from 18 to 78 days from Ke-Macina to Dire (Olivry, 1995). The annual losses by evaporation reach 48% of the water inputs during the wet period and only 24% during the dry period (Mahe *et al.*, 2009).

The Delta can be divided into two distinct geomorphological entities: the Upstream Delta (USD) a traditional flood plain extended from the south to the central lakes (Debo Lake, Fig. 1), the downstream Delta (DSD in the northern of the central lakes, is a series of flooded ergs (erg of Niafunke). The studied window (Fig. 1) located in the USD is about 31 682 km^2.

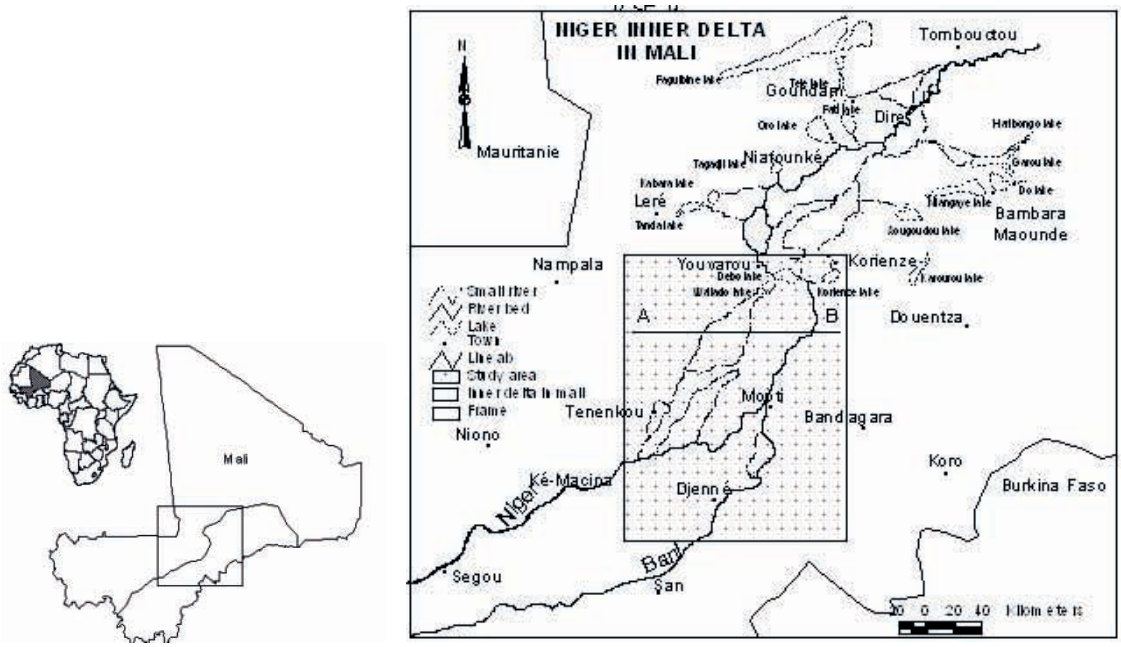

Fig.1 Location of the Niger Inner Delta in Mali, and extraction window of the studied images.

DATA AND METHODOLOGY

We used four images, collected at various dates, of the mean hydrological phases of the flood in the NRID: 22 February 1999 (beginning of low flows), 9 June 1999 (low flows minimum), 18 October 1999 (flood maximum in the USD) and 1 December 1999 (flood maximum in the DSD). Cloud-free images with NRID to nadir are selected. The studied period extends over two hydrological cycles 1998–1999 and 1999–2000, beginning in May. These two annual cycles correspond to 3880 m^3 s^{-1} and 4080 m^3 s^{-1} annual flows, respectively. The row AVHRR images data (in numerical count), comprises five spectral bands: bands 1 (visible) and 2 (near infra-red); the thermal bands 3 (middle infrared), 4 and 5 (infra-red thermal). The images must be radiometrically and geometrically pre-processed before retrieval of the Normalised Difference Vegetation Index (NDVI) by a simple arithmetic transformation of the two first bands (difference between bands B1 and B2 (visible) standardized by their sum).

FLOODED ZONES DISCRIMINATION FROM THE MULTISPECTRAL DATA

Many methods of delimitation of open water surfaces from optic (reflective and thermal domain) and active microwaves (C and L bands) exist in the literature, for instance, visual analysis coupled with the spectral analysis in the Sahelian zone (Thiam & Ovtracht, 1998; Crétaux *et al.*, 2011), method of thresholding applied to the histogram (Mcfeeters, 1996; Verdelta, 1996) and the ratio of the bands (Rigal, 1989; Wald, 1990; Bo-Cai, 1996; Mcfeeters, 1996, Bryant & Rainey, 2002). Methods of spectral adjustment and spectral unmixing (Bajjouk *et al.*, 1998; Drake *et al.*, 1999), rules of discrimination based on simple logical expressions (Richard & Jia, 1999) were used for mapping the flooded areas. All these methods are based on the analysis of the spectral signatures related to the nature of the items observed and the characteristics of the sensors. Comparison of the spectral signatures of several objects: sandy soils, water and vegetation, between the ground truth (Fig. 2(a)) and the $AVHRR_{14}$ sensor records (1 km resolution) (Fig. 2(b)) show that the building of indexes based on ratios of bands for items recognised on the surface is possible.

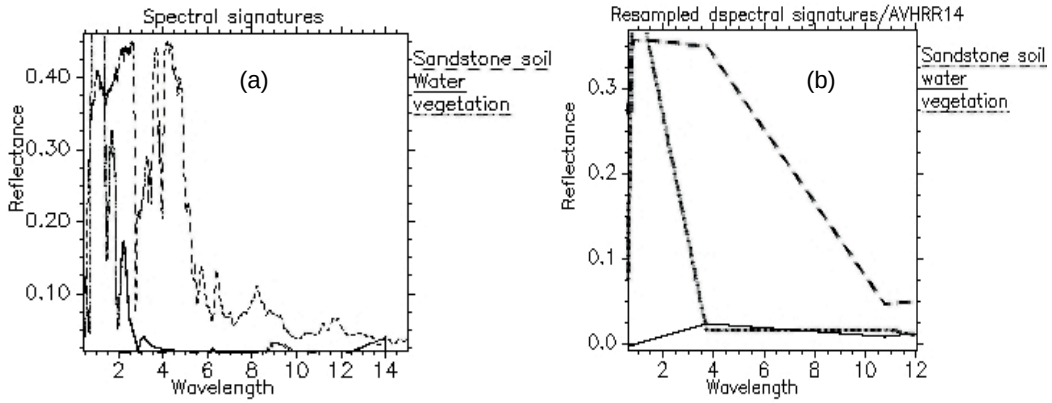

Fig. 2 Comparison of the spectral signatures of several objects: sandy soils, water and vegetation, between the ground truth (a) and the AVHRR14 sensor records (b).

Table 1 Different indexes found in the literature.

Indexes	Type of data	References	Actual using
$NDVI = (NIR - RED)/(NIR + RED)$	AVHRR AVIRIS TM	Rigal, 1989 Bo-Cai, 1996 Dale *et al*, 1997	$NDVI=(B_2-B_1)/(B_2+B_1)$
$NDWI = (GREEN - NIR)/(GREEN + NIR)$	LANDSAT MSS	McFeeters, 1996	$NDWI=(B_1-B_2)/(B_2+B_1)$
$J = (IR - NIR)/(IR + NIR)$	AVHRR	Rigal, 1989	$J=(B_5-B_2)/(B_5+B_2)$
R_c	AVHRR	This study	$R_c=B_4/B_2$
IB_T	AVHRR	This study	$IB_T=\sqrt{(B_3^2+B_4^2+B_5^2)/3}$

NDVI, Normalized Difference Vegetation Index; GREEN, Green channel; NDWI, Normalized Difference Water Index; RED, Red channel; J, Index of presence of water; NIR, Near infrared; R_c, Channel ratio; IR, Infrared; IB_T, Thermal Brightness Index.

In the NRID area, distinction between flooded vegetation and vegetation on dry soils is a challenge. Some indexes found in the literature (Table 1) are tested and confronted with new indexes in this study. Selected indexes are applied for two extreme periods (June and December) of the annual hydrological cycle of the NR to discriminate open water, flooded vegetation, vegetation on dry soil and bare soils. On the off-water areas, the distinction between soils covered

by vegetation and bare soils is difficult when using grey levels images. We thus grouped them under the term of "off-water soils".

Table 2 gives the characterisation of the spectra along profile AB (Fig. 3) in grey levels and in positive or negative value of the numerical account compared to the average. That gives a qualitative description of the spectral behaviour of the above-mentioned geographical items according to time, for each spectral index. In Fig. 3, we represent the spectral signatures according to the AB profile and the corresponding image in grey levels. The flooded vegetation appears in white on grey level images, and is more marked for dense vegetation. In December the off-water areas appear in light grey because of its low vegetation cover rate.

Table 2 Comparative study of various indexes using grey levels (NG) images with numerical accounts (CN) for two periodes: at the end of the dry season (lowest flood level, June 1999), and at the end of rainy season (maximum flood level, December 1999).

Objects / Indexes	9 June 1999								1 December 1999					
	Inundation flood plain						Dry soils		Inundation flood plain				Dry soils	
	Open water		Vegetalized soils		Bare soils				Open Water		Vegetalized Water			
	NG	CN	NG	CN	NG	CN	NG	CN	NG	CN	NG	CN	NG	CN
NDVI	b	–	w	+	g	–	g&w	±	b	–	w	+	gw	avl
NDWI	w	+	b	–	w	+	g	+	w	+	b	–	gw	avl
J	w	+	w	+	w	+	gb–gw	–	w	+	gb	–	g	–
R_c	w	+	w	+	w	+	gb–gw	–	w	+	g b	–	g b	–
IB_T	b	–	gw	+	gw	+	g	+	b	–	b	–	gw	+

NG, grey levels (w: white; b: black; g: grey; gb: grey to black; avl: average level); CN, level of the numerical account in regard to, the average (+: positive; –: negative).

The NDWI (Bo-Cai, 1996) and J (Rigal, 1989) indexes are built according to the same principle: a standardized difference between respectively the bands B1–B2 and B5–B2 (Table 1). They both present the higher numerical values for open water (Fig. 3). The value of the J index is higher than that of the NDWI; it implies stronger contrasts between open water and soil covered by vegetation (Table 2). The R_C index also presents strong amplitudes for open water. The index of brightness IB_T in thermal spectrum shows a large difference between bare soils (CN > 200) and flooded surfaces (CN = 190), being a good index for the flooded areas.

To conclude: (i) the NDWI index appears to be a good index for open water (in grey level) either in periods of low flows or peak flood; (ii) the R_C and J indexes present similar results in periods of floods, with a better contrast for the interface between open water and off-water soil. In period of low flows, the contrast between the flood plain soils and the all-time off-water soils remains well marked; (iii) the index of brightness in the thermal spectral (IB_T) is a very good index of the presence of water appearing in black. However, confusion between open water and flooded vegetation, and wet soils, appears in December.

Consequently, the indexes tested highlight in a more or less clear way the simple items such as bare soil, open water or soils covered by vegetation. But none makes it possible to identify the occurrence of the complex object of flooded vegetation. Its identification needs application of several indexes and composite image analysis.

COLOUR COMPOSITE IMAGES ANALYSIS

The most relevant indexes according to the objectives of this study, IB_T, NDVI and R_C (Fig. 3), are used for the colour composite images (Fig. 4). The index of brightness (IB_T), a very good indicator

Indexes tested	Spectral response	Image in grey-scale (B/W) June 1999	Spectral response	Image in grey-scale (B/W) December 1999
NDVI	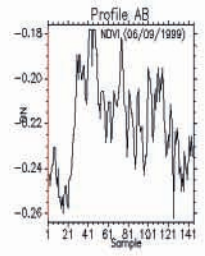	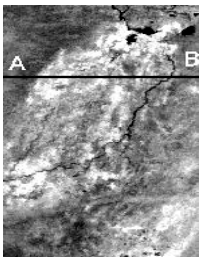	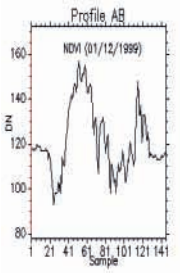	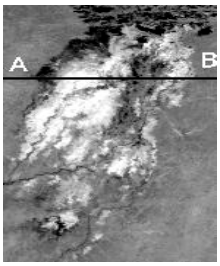
NDWI	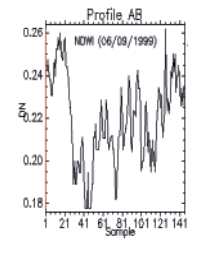	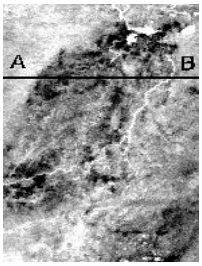	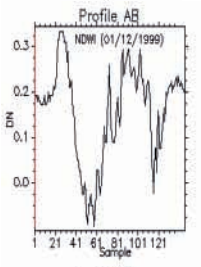	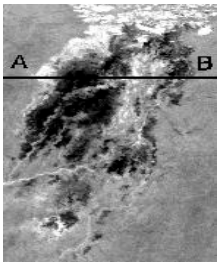
J	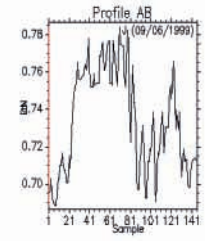	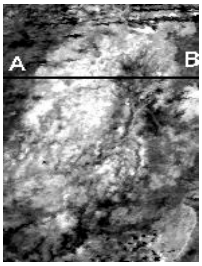	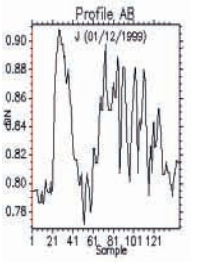	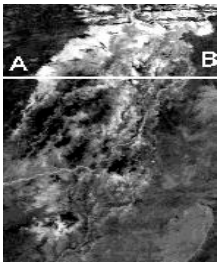
R_c	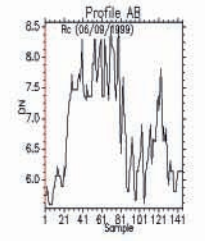	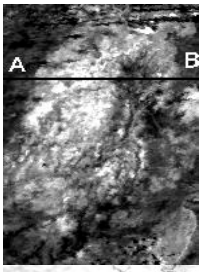	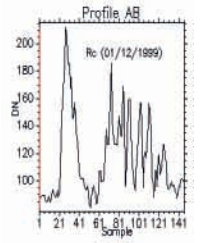	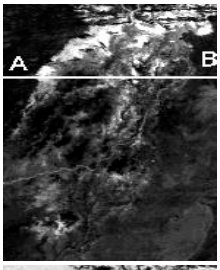
IBt	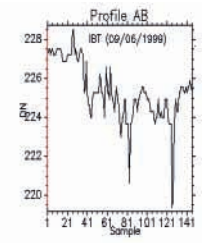	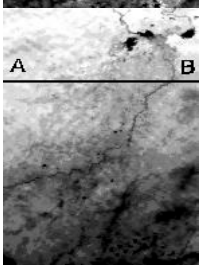	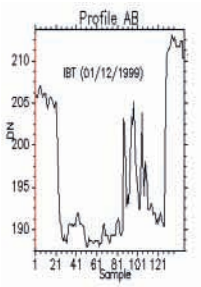	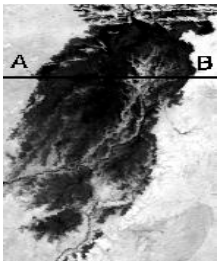

Fig. 3 Evolution of grey levels between an image taken in dry season (June 1999, left) and an image taken during the flood (December 1999, right), according to the indexes NDVI, NDWI, J, Rc and IBt.

of the presence of water and its absence, i.e. in dry soils, is presented as a red colour. The NDVI index (green), allows monitoring the vegetation cover either on flooded or on off-water areas. The R_C index (blue) allows a better discrimination between the open water and the soil than the NDWI. The geographical areas identifiable in NRID are:

(a) Open water areas: appear in dark blue in the DSD. It is possible to distinguish the river bands, the flood plains and the peripheral lakes. In the USD, the open water areas are visible on the

borders of the vegetation zones, and probably correspond to the areas lately filled by water; the absence of blue colour for the BR would be related to the narrowness of the river compared to the spatial resolution of the NOAA/AVHRR sensor;

(b) Open water areas appear dark blue (in DSD) in river channels, flood plains and peripheral lakes. The open water visible on the borders of the vegetation zones (in USD), is probably the latest areas filled by water; the absence of blue for the BR would be related to the narrowness of the river compared to the NOAA sensor spatial resolution (1 km).
(c) Flooded vegetation zones are presented as a green olive colour, becoming cyan in DSD;
(d) Vegetation on dry soil in yellow towards the north is primarily grassy formations on sandy soils; towards the south, increasingly green colour shows the abundance of vegetation at that time (December 1999);
(e) Bare soil zones: reddish to orange colour, appear in the Delta only on one small area near the Mayo Dembe River in a north–south direction (Fig. 4) and in the septentrional part along old fixed or recent sand dunes in a northwest direction.

FLOODING WAVE PROPAGATION

Colour composite images corresponding to the four main stages of the annual hydrological cycle are analysed to describe the flooding wave propagation (Fig. 5). The image from February corresponds to a phase of intensive draining of the flooded plains. The three other images (in June, October and December) represent the phases of drying, water rising and maximum flooding in the USD, respectively.

Flood propagation speed depends on the annual peak flow. In the USD basin, the propagation occurs from 2 to 6 days, between Koulikoro (60 km from Bamako) to Ke-Macina, entry of the Delta, 300 km downstream. Within the Delta, the transfer time is largely variable. Between Ke-Macina and Mopti, it takes 3–19 days. The section Mopti-Akka (exit of the Debo Lake in the centre part of the Delta) requires 15–35 days, and in DSD, the transfer time varies between 2 and 14 days from Akka to Dire (exit of the Delta). These delays are exceeded during wetter years. So the propagation time of the water rising can be estimated as 20 to 80 days across the all NRID.

The spectral behaviour analysis along profile A–B allows monitoring the propagation of the various floods described above. On the whole cycle the open water appears (dark blue colour) in the Debo, Wallado and Korientze lakes. Elsewhere, open water is rare in February, except in the major bed of the NR and in its main effluents. In June, open water is only visible in the centre of the Debo Lake and in the major bed of the NR. In October, water settles significantly everywhere to reach its maximum level in December, shown by a great overflow in the northern part of the USD (Fig. 5). On profile A–B, the frame of the spectrum IB_T marked by low values describing a low flat curve, confirms the presence of water under the vegetation cover.

The primarily herbaceous vegetation (from green to red colour) starts its degradation in February due to a lack of water, senescence and mainly to the return of the livestock. In June the vegetation cover thus mainly disappears to leave a naked soil with colour from reddish to yellowish on the off-water soils from the north, and with a violet colour in the flood plain indicating a probable presence of moisture. In the south the off-water areas appear in green colouring because of the combined effect of the rain (beginning of the rainy season) and of the presence of clouds disturbing the signal acquirement. In October and December, the vegetation remains abundant in flooded and off-water areas.

These changes of colours on the colour composite images from one period to another, show that the behaviour corresponding to the open water (blue), the vegetation (green), the bare soil never flooded (in reddish to yellowish) and the bare soil of the flood plain (in purple), established according to pseudo-bands $IB_{T,}$ NDVI and R_C, is in accordance to the observed propagation of the flood. The colorimetric characteristics of the broad topics of soil occupation calculated from this visual analysis of the colour composite images are presented in Table 3.

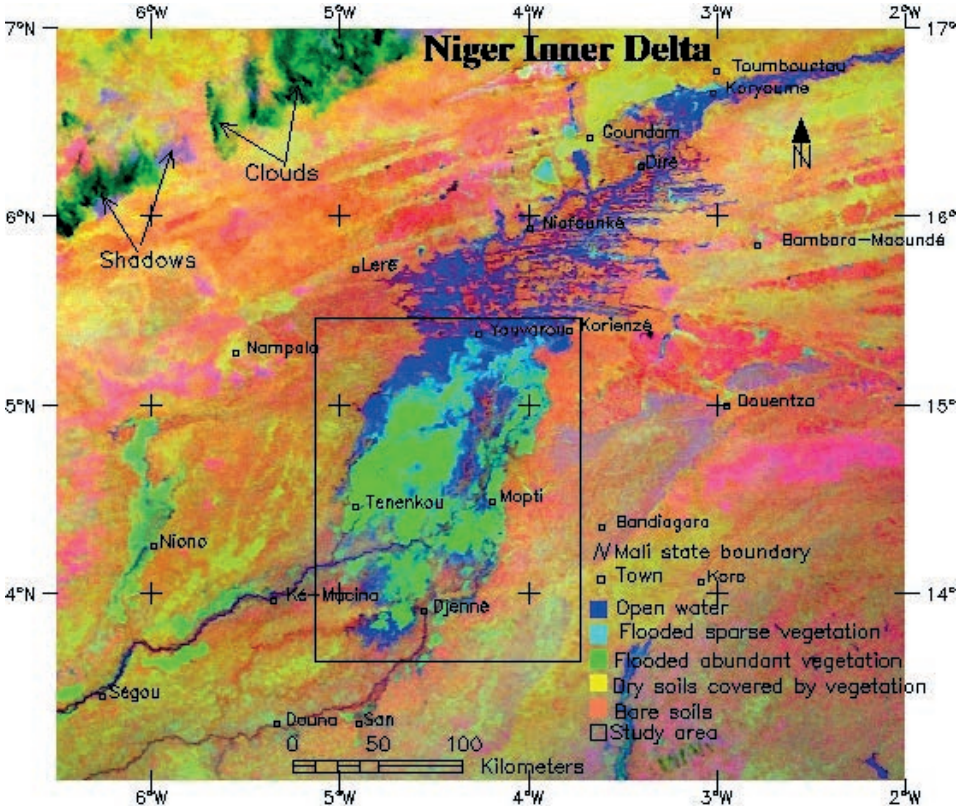

Fig. 4 Colour composite images of the NRID during the flood period (December 1999), from indexes IB_T (Red), NDVI (Green) and R_c (Blue).

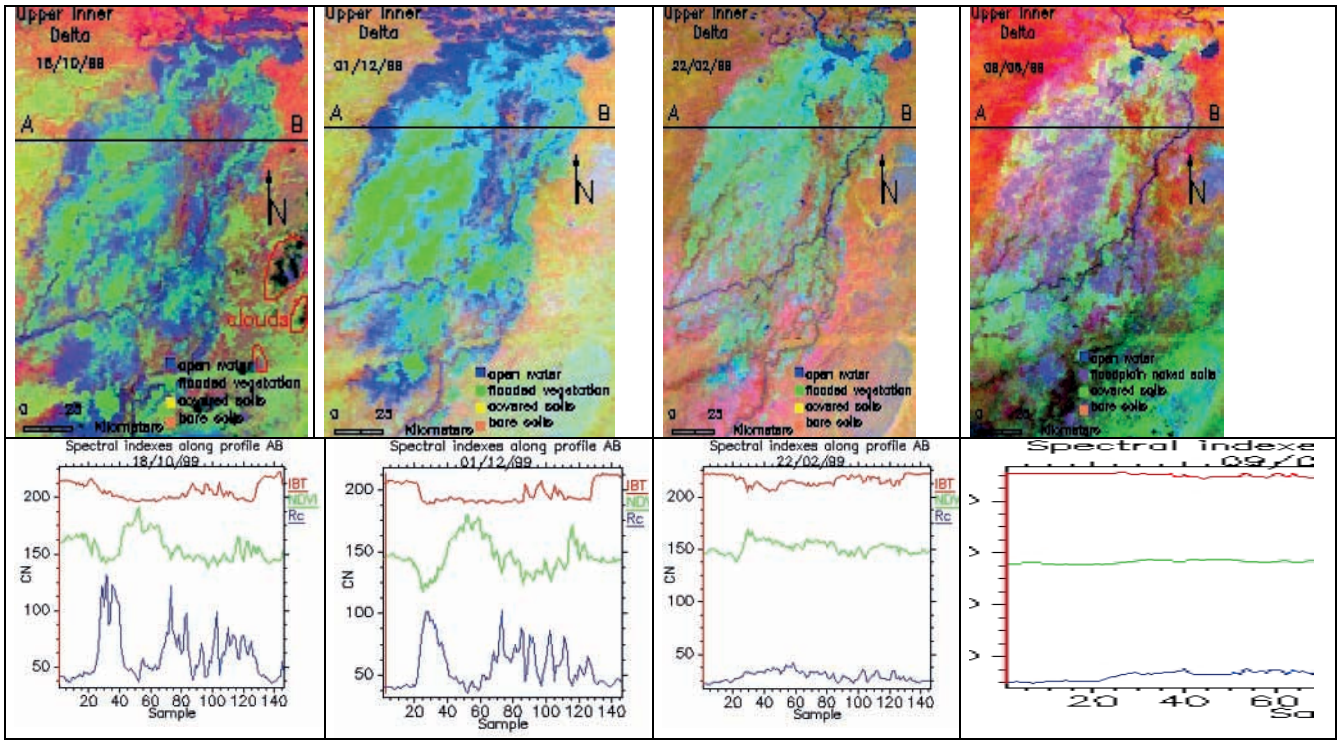

Fig. 5 Flood spatial-temporal dynamics after colour images (from indexes IB_T (red), NDVI (green) and R_c (blue)), of the USD, showing four major phases of the annual flooding cycle, and location of the A–B profile for the comparative study.

Table 3 Visual analyses of the colour composite (from pseudo-bands IB_T (red), NDVI (green) and R_c (blue)) representing a complete inundation cycle in the NRID.

Date of the colour composite images	Calorimetric characteristics of the main types of land				
	Open Water	Flooded Vegetation	Bare soils	Bare soils within the flood plain	Dry soils with vegetation
22 February 1999	Dark blue	Green olive and light green dominate	Reddish		Yellow dark red to pink
9 June 1999	Dark blue	Green olive and darker southward	Reddish	Purple	Yellow dark red to dark green
18 October 1999	Dark blue	Green olive	Reddish		Yellow dark red to green
1 December 1999	Dark blue	Green olive becoming cyan towards north	Reddish		Yellow greenish

CONCLUSION

The indexes applied to the AVHRR data, allow discrimination of the various geographical items composing the landscape of the NRID flood plain, i.e. the open water, the flooded vegetation, the vegetation on dry soil and the bare soils. Indeed the indexes suggested allow detection of water occurrence under a dense herbaceous cover in Sahelian wetland zone.

The colour composite images must be built from: Index of the Brightness in the thermal spectral (IB_T), which is very sensitive to moisture, the NDVI for it description of the vegetation cover and the index R_C, ratio of channel 4 (thermal) on channel 2 (visible) sensitive to open water. These indexes are powerful tools for flood mapping and flood propagation monitoring in the NRID on a kilometre scale, from NOAA data.

Acknowledgements This research was initiated by the GIHREX program (Natural resources integrated management in the RNID) of IRD. It is the subject of a doctoral thesis of the University of Montpellier II, Programme Vahyne, UMR Hydrosciences, with the financial support of the French Cooperation Services in Mali, and the technical and scientific support of Agrhymet in Niamey. I would like to acknowledge Andre Nonguierma, previously GIS Officer at Agrhymet, for reviewing this manuscript.

REFERENCES

Bajjouk, T., Populus, J. & Guillaumont, B. (1998) Quantification of subpixel cover fractions using principal component analysis and a linear programming method: application to the coastal zone of Roscoff (France). *Remote Sensing of Environment* 64(2), 153–165.

Bo-Cai, G. (1996) NDWI A normalized difference water index for remote sensing of vegetation liquid water from space. *Remote Sensing of Environment* 53(3), 257–266.

Bryant, R. G. & Rainey, M. P. (2002) Investigation of flood inundation on playas within the Zone of Chotts, using a time-series of AVHRR. *Remote Sensing of Environment* 82, 360–375.

Conway, D. & Mahé, G. (2009) River flow modelling in two large river basins: the Parana (subtropical) and the Niger (tropical). *Hydrological Processes* 23(22), 3186–3192.

Crétaux, J. F., Bergé-Nguyen, M., Leblanc, M., Abarca Del Rio, R., Delclaux, F., Mognard, N., Lion, C., Kumar Pandey, R., Tweed, S., Calmant, S. & Maisongrande, P. (2011) Flood mapping inferred from remote sensing data. *International Water Technology Journal* I(1), June 2011, 46–58.

Drake, N. A., Mackin, S. & Settle, J. J. (1999) Mapping vegetation, soils and geology in semiarid shrublands using spectral matching and mixture modeling of SWIR AVIRIS Imagery. *Remote Sensing of Environment* 68(1), 12–25.

Jackson, R. D. (1983) Spectral index in N-space. *Remote Sensing of Environment* 5, 5, 999–1021.

Justice, C. O. & Hiernaux, P. H. Y. (1986) Monitoring the grasslands of the Sahel using NOAA AVHRRR data: Niger 1983. *Int. J. Remote Sensing* 7(11), 1475–1497.

Lienou, G., Mahé, G., Dieulin, C., Paturel, J. E., Bamba, F., Sighomnou, D. & Dessouassi, R. (2010) The river Niger water availability: facing future needs and climate change. In: *Global Change: Facing Risks and Threats to Water Resources* (Proc. of the Sixth World FRIEND Conference, Fez, Morocco, October 2010), 637-645. IAHS Publ. 340. IAHS Press, Wallingford, UK.

McFeeters, S. K. (1996) The use of the normalized difference water index (NDWI) in the delineation of open water. *Int. J. Remote Sensing* 17, 1425–1432.

Mahé, G., Bamba, F., Soumaguel, A., Orange, D. & Olivry, J. C. (2009) Water losses in the Niger River Inner Delta: water balance and flooded surfaces. *Hydrological Processes* 23(22), 3157–3160.

Mahe, G., Lienou, G., Bamba, F., Paturel, J. E., Adeaga, O., Descroix, L., Mariko, A., Olivry, J. C. & Sangare, S. (2011) Niger river and climate change over 100 years. In: *Hydro-climatology: Variability and Change* (ed. by S. W. Franks *et al.*). Proceedings of symposium J-H02 held during IUGG2011 in Melbourne, Australia, July 2011, 131–137 IAHS Pub. 344. IAHS Press, Wallingford, UK.

Mulligan, M., Saenz Cruz, L.L., Pena-Arancibia, J., Pandey, B., Mahe, G. & Fisher, M. (2011) Water availability and use across the Challenge Program on Water and Food (CPWF) basins. *Water International* 36(1), 17–41.

Ogilvie, A., Mahé, G., Ward, J., Serpantié, G., Lemoalle, J., Morand, P., Barbier, B., Diop, T., Caron, A., Namarra, R., Kaczan, D. , Lukasiewicz, A., Paturel, J. E., Liénou, G. & Clanet, J. C. (2010) Water, agriculture and poverty in the Niger River basin. *Water International* 35(5), 594–622.

Olivry, J. C. (1995) Fonctionnement hydrologique de la cuvette lacustre du Niger et essai de modélisation de l'inondation du Delta intérieur. In: Grands bassins fluviaux péri atlantique (ed. by J. C. Olivry & J. Boulègue), 267–278. Colloques et Séminaires ORSTOM, Paris.

Poncet, Y. & Orange, D. (1999) L'eau, moteur de ressources partagées: l'exemple du Delta intérieur du Niger au Mali. *Aménagement et Nature* 132, 97–107.

Richard, J. A. & Jia, X. (1999) *Remote Sensing Digital Image Analysis*, 3rd edn. Springer, New York.

Rigal, D. (1989) Crue et décrue au lac Tchad, Essai de suivi a partir des images NOAA, novembre 1988-avril 1989. *Veille Climatique Satellitaire* 28, 71–76.

Smith, M. O., Pierce, L. L., Running, S. W. & Gillepsi, A. R. (1990) Vegetation in deserts: 1. A regional measure of abundance from multispecral images. *Remote Sensing of Environment* 31, 1–26.

Thiam, S. & Ovtracht, N., (1998) Suivi des écosystèmes du Delta Intérieur du Niger à partir des données spots (région de Mopti – Mali). *Photo-Interpretation* no. 2–3.

Townshend, J. R. & Justice, C. O. (1986) Analysis of the dynamics of African vegetation using the normalized difference vegetation index. *Int. J. Remote Sensing* l7(11), 1435–1445.

Verdelta, J. P. (1996) Remote sensing of ephemeral Water bodies in western Niger. *Int. J. Remote Sensing* 17(4), 733–748.

Wald, L. (1990) Monitoring the decrease of Lake Chad from space. *Geocarto International* 5(3), 31–36.